SDC 92-223
ANL-HEP-TR-92-22

# Simulation of Hanging File Experiments with CALOR89 [1]

*P.K. Job, L.E. Price and J. Proudfoot*
*Argonne National Lab, Argonne IL 60439*
*T. Handler*
*University of Tennessee, Knoxville TN 37996*
*T.A. Gabriel*
*Oak Ridge National Lab, Oak Ridge, TN 37831*

ANL-HEP-TR--92-22
DE92 014766

## 1. Introduction

This note presents the comparison of CALOR89 simulation with the 'hanging file' test measurements conducted at Fermilab during the period of Sep 91- Jan 92 . The purpose of this study is to benchmark CALOR89 code against the experimental data to enhance it's reliability and predictive power. Seven hanging file configurations were simulated. The measured values of e/$\pi$ ratio (the ratio of electron to pion signal at the same energy), hadronic and electromagnetic resolutions were compared with the simulations. The depth profiles of the hadronic and electromagnetic showers are also compared.

The simulated configurations are the following;

1. (1/8"Pb+scin)*40 cells, (1"Pb+scin)*52 cells
2. (1/8"Pb+scin)*40 cells, (1"Fe+scin)*55 cells
3. (3/4"Pb+scin)* 92 cells
4. (3/4"Fe+scin)* 90 cells
5. (1"Fe+scin)* 69 cells
6. (3/4"Pb+1/16"Al+scin+1/16"Al)* 50 cells, (3/4"Pb+scin)* 42 cells
7. (3/4"Fe+1/16"Al+scin+1/16"Al)* 50 cells, (3/4"Fe+scin)* 40 cells

In all the configurations the scintillator thickness was 0.30cm.

[1]Work supported in part by US Department of Energy, Contract No. W-31-109-ENG-38, No. DE-AC05-84OR21400 and No. DE-AS05-ER03956

The parameters of CALOR89 optimized in an earlier study[1] is used in these simulations. The ESKALE[1] value used is 15 GeV. This can cause a systematic error in the simulations at energies $\leq$ 20 GeV. The maximum systematic error in the hadronic resolution will be at the particle energy of 15 GeV and will be of the order of $\sim$3%. The shower integration time used for all the simulations is 96 nsec, which is used in the hanging file measurements. The hadronic resolution as a function of shower integration time is studied only for configuration 5.

## 2. Non-Homogeneous Configuration

The configurations 1 and 2 are non-homogeneous. These configurations have separate electromagnetic and hadronic sections. In such inhomogeneous configurations the hadronic signal from the two segments are weighted by a scheme which minimizes the hadronic resolution. One such scheme used in the earlier studies was based on minimum ionizing dE/dX. This scheme was found inadequate. Therefore a scheme based on an optimized weight factor is chosen.

$(\text{Signal})_{TOT} = (\text{Signal})_{EM} + \alpha \times (\text{Signal})_{HAC}$

where $\alpha$ is chosen such that the resolution is a reasonable minimum at all particle energies.

Figure 1 gives the resolution for configuration 1 as a function of the weight factor ($\alpha$). The optimum weight factor chosen for this configuration in the hanging file experiment was 5.5 whereas the dE/dX weight factor is 7.1. Similarly figure 2 gives the resolution for configuration 2 as a function of $\alpha$. In this case the weight factor chosen by the hanging file experiment was 4.5 and the dE/dX weight factor is 6.5. It can be observed that the dE/dX weight factor is a good approximation for the system with lead in the hadronic section (conf.1) whereas it is a poor approximation for the system with iron in the hadronic section. The results also show that in either case it is difficult to choose a unique weight factor such that the hadronic resolution is minimum at all energies. This can have implications for jet resolution wherein the individual particles are not resolved.

Figure 3 gives the hadronic resolutions calculated by CALOR89 for the two configurations (1 and 2) corresponding to the weight factors optimized by the hanging file experiments. The resolutions are plotted as a function of inverse squareroot of the particle energy. The resolution data points at different energies are fitted using a $\chi^2$ fit to a functional form;

$(\sigma/E)^2 = (a^2/E) + b^2$

The fits for these configurations are given as

configuration 1$\Rightarrow$ $54.17/\sqrt{E}\oplus$ 5.15 ($57.17/\sqrt{E}\oplus$ 4.9)

configuration 2$\Rightarrow$ $61.55/\sqrt{E}\oplus$ 6.25 ($51.00/\sqrt{E}\oplus$ 3.7)

The values in parenthesis are the measured resolutions from the hanging file experiments. The statistical errors on the simulated coefficients are 2% on the stochastic term and 0.5% on the constant term.

The results show that there is a reasonable agreement between simulation and experiment in the case of configuration 1. But in the case of configuration 2, where hadronic section is made up of iron, there is considerable disagreement between simulation and the measurement. This problem is under active investigation. It can also be seen that the resolution corresponding to the energy 15 GeV is not fitting the pattern due to the choice of the ESKALE value. Calculations were repeated by changing the ESKALE value to 10 GeV and 5 GeV. The resolution values were lower by 4% for both the configurations which is the maximum error due to the choice of the ESKALE. It was also noticed that at 15 GeV particle energy the choice of ESKALE as 5 GeV or 10 GeV did not make a difference. Thus our estimated systematic error due to the choice of the ESKALE value as $\pm 3\%$[1] seems reasonable.

Figure 4 gives the simulated electromagnetic resolution as a function of energy for configurations 1 and 2. These resolution values can be fitted to a form

$12.2/\sqrt{E}\oplus$ 0.06

This agrees well with the experimental measurements when corrected for the systematic errors. The near zero constant term maker it a good candidate for the SDC electromagnetic calorimeter.

## 3. Homogeneous Configurations

Configurations 3,4 and 5 are homogeneous. For these the e/$\pi$ ratio, hadronic and electromagnetic resolutions are estimated by CALOR89. The intrinsic e/h ratio for these configurations (the ratio of electron to pure hadron signal of the same energy) is also estimated by CALOR89. The results of the e/$\pi$ and e/h analysis for the three homogeneous configurations are given in figure 5. The results of the hanging file measurements are given for comparison. The CALOR89 estimated e/$\pi$ ratio for homogeneous lead configuration and for homogeneous iron configuration agrees remarkably well with the measurements. For the homogeneous iron configuration the CALOR89 estimated e/$\pi$ ratio tends to be non-linear by 15% at 10 GeV whereas the measured value shows much less non-linearity. The e/$\pi$ ratio reported earlier for a similar system[2] shows a non-linearity of 12 to 15% in the particle energy range of 10 to 140 GeV. The e/h ratio is linear with respect to energy as expected. The slight non-linearity in the iron case could be due to the transverse dimensions of the test module, since the hadronic showers tend to be of much larger transverse dimensions in iron systems. Physics considerations tell us that the e/$\pi$ ratio is approximately equal to e/h at low energies and tends to be 1.0 at high energies.

Figure 6 gives the hadronic resolution as a function of energy for the three homogeneous configurations. These resolution values can be fitted to the above functional form and the fits are given as

configuration 3$\Rightarrow$ $52.44/\sqrt{E}\oplus$ 0.60 ($51.70/\sqrt{E}\oplus$ 3.2)

configuration 4$\Rightarrow$ $62.02/\sqrt{E}\oplus$ 3.80 ($45.40/\sqrt{E}\oplus$ 3.9)

configuration 5$\Rightarrow$ $63.43/\sqrt{E}\oplus$ 4.20 ($57.30/\sqrt{E}\oplus$ 3.0)

The values in parenthesis are the measured resolutions from the hanging file experiments. The statistical errors on the simulated coefficients are 2% on stochastic term and 0.5% on constant term.

The stochastic term for the homogeneous 3/4" lead-scintillator configuration(conf.3) agrees well with the measurements. The simulation predicts a much smaller constant term whereas the measured constant term is much larger. The constant term

reported from an earlier measurement[3] with a test module of 1.0cm lead plates followed by 0.25cm of scintillator plates is 1.3 (this calorimeter was only 5$\lambda$ in depth).The linearity of the lead-scintillator system also dictates a smaller constant term. The resolution values predicted by CALOR89 for the 1" iron system(conf. 5) agrees reasonably well with the experimentally measured value. However the CALOR89 predictions for the 3/4" iron system (conf. 4) is quite different compared to the measurements. CALOR89 predicts negligible improvement in resolution from 1" to 3/4" iron plates whereas the measurement shows almost 20% improvement. The previously reported experimental hadronic resolution for such a system[2] is $58/\sqrt{E}$ which is closer to the CALOR89 prediction.

The hadronic resolution as a function of shower integration time was estimated by CALOR89 for the configuration 5. The results are given in figure 7. The range of shower integration gate studied is 16 to 500 nsec. It shows that for the iron-scintillator systems the shower integration gate play a non-significant effect on the hadronic resolution. The variation in hadronic resolution is within the statistical errors. This is in agreement with the conclusion reported by the hanging file measurements for the same configuration.

The electromagnetic resolutions for the three homogeneous configurations are given in figure 8. The fitted coefficients are given as

configuration 3$\Rightarrow$ $33.21/\sqrt{E}\oplus$ 0.90

configuration 4$\Rightarrow$ $21.69/\sqrt{E}\oplus$ 0.90

configuration 5$\Rightarrow$ $24.58/\sqrt{E}\oplus$ 0.60

At present the electromagnetic resolution values for the complete energy range for the above configurations are not available from the hanging file experiments. The reported value for a configuration similar to conf.4 is $23.0/\sqrt{E}$[2] which agrees well with our simulation. The constant term is less than 1% for all these configurations. Detailed comparisons will be done as soon as the complete set of experimental values are available.

## 4. Cladded Scintillator Configurations

Configurations 6 and 7 have some of the scintillator plates cladded with 1/16" aluminium. The purpose of this study was to compare the effect of scintillator cladding on the calorimeter parameters. It was also interesting for us to check the reliability of CALOR89 predictions for systems with very thin layers of material. It has been observed earlier[4][5] that the properties of the thin layer configurations ($\leq$1mm) are sensitive to the EGS input parameters like the multiple scattering step size and the energy cuts(the energies at which the particle histories are terminated).

Table I gives the summary results of these simulations. The parameters for the uncladded configurations are also given for comparison. Two calculations were repeated with low energy cuts in EGS4 (200 keV for electrons and 10 keV for photons). The results show that the 1/16" aluminium cladding has a non-negligible effect on the $e/\pi$ ratio for the lead configuration whereas the cladding has no effect for the iron configuration. The effect of cladding on the electromagnetic and hadronic resolutions is negligible for both the configurations. The calculations with low energy cuts in EGS4 did not show any significant effects which proves that the 1/16" scintillator cladding can be simulated with the normal input parameters of EGS[4]. These results are also verified by the hanging file experiments.

## 5. Depth Profiles of Hadronic Showers

Figures 9 and 10 gives the typical depth profiles for the 3/4" iron-scintillator configuration. The solid histograms are the simulated profiles and the dotted the hanging file measurements. The particle energies are 25 GeV and 100 GeV. The events which deposits $\geq$95% of the energy in the first 20 radiation lengths of the calorimeter are rejected. These were typically $\leq$1% of the events. The two histograms are normalized such that the total energy is conserved. The figures show that the agreement is good for both the energies. The CALOR89 profiles have a slight tendency to fall quicker than the measurements. But the overall agreement is quite desirable.

Figures 11 and 12 gives the typical normalized depth profiles for 25 and 100 GeV pions for the 3/4" lead-scintillator configuration. The agreement is good at 25 GeV. But the agreement is not so good for 100 GeV. We observe a double peak in the simulated distribution at 100 GeV and also at higher energies. This could be due to an error in the simulation of the first collision. It can also be statistical such that the peaks disappear when sufficient number of events are simulated. This point is under investigation.

## 6.Conclusions

The results show that the CALOR89 can predict reasonably well the test beam measurements with the scintillating plate calorimeters. The agreement in the case of lead-scintillator homogeneous configuration is excellent in terms of the $e/\pi$ ratio and the hadronic resolution. It could predict reasonably well the outcome of iron-scintillator homogeneous configurations. These results are also in agreement with the previous measurements. In the case of two segment non-homogeneous configurations, the resolutions were optimised by a single weight factor for all energies. The agreement between CALOR89 simulation and the measurement in this case is good when both the segments consist of the same absorber material, lead. There is considerable disagreement for the configuration with different absorber materials like lead and iron. This point needs further investigation. CALOR89 could also predict the shower depth profiles reasonably well in the three homogeneous configurations.

## Acknowledgements

The authors wish to acknowledge with thanks the cooperation and help given by the hanging file experimental group, especially by Dr.G.W. Foster and Dr.A.Byon of Fermilab, by providing before publication the hanging file experimental results for comparison with CALOR89 simulations.

## References

[1]. P.K. Job et al.,Comparison of CALOR89 model predictions with scintillator plate calorimeter data, Nucl.Instr.and Meth., A309(1991)60.

[2] H. Abramowicz et al., Response and Resolution of a Iron- Scintillator Calorimeter, Nucl.Instr.Meth. 180(1981)429.

[3] E. Bernardi et al., Performance of a Compensating Lead- Scintillator Hadronic calorimeter, Nucl.Instr.Meth. A262(1987)229.

[4] P.K. Job, G. Sterzenbach and D. Filges, Optimization of EGS Parameters, Nucl.Instr.Meth. A271(1988)442.

[5] D.W.O.Rogers, Low Energy Electron Transport with EGS, Nucl.Instr.Meth.A227 (1984)535

**Table I**

**Summary Results for Cladded Scintillator Configurations (10 GeV pions and electrons)**

| Configuration | e/$\pi$Ratio | EM Resolution ($\sigma$/E) | Had. Resolution ($\sigma$/E) |
|---|---|---|---|
| Pb/Scin 1.9/0.30cm | 0.95±0.01 | 10.77±0.76 | 18.89±0.54 |
| Pb/Al clad Scin 1.9/.16/.3/.16cm | 0.92±0.01 | 11.10±0.51 | 19.19±0.53 |
| Pb/Scin low cuts in EGS | 0.96±0.01 | 10.70±0.62 | 20.26±0.62 |
| Pb/Al clad Scin low cuts in EGS | 0.93±0.01 | 10.50±0.62 | 19.45±0.58 |
| Fe/Scin 1.9/0.30cm | 1.35±0.01 | 6.92±0.51 | 20.71±0.74 |
| Fe/Al clad Scin 1.9/.16/.3/.16cm | 1.35±0.01 | 6.61±0.33 | 21.14±0.53 |

**List of figures**

1. Hadron resolution as a function of weight factor for the lead-scintillator two segment calorimeters.

2. Hadron resolution as a function of weight factor for the lead-scintillator and iron-scintillator two segment calorimeters.

3. Hadron resolution as a function of inverse squareroot of energy for the two segment non-homogeneous configurations.

4. Electromagnetic resolution as a function of inverse squareroot of energy for the lead EMC test configuration.

5. The e/h and the $e/\pi$ ratio as a function of energy for the three homogeneous test configurations. (solid curves are $e/\pi$ and the dashed e/h)

6. Hadron resolution as a function of inverse squareroot of energy for the three homogeneous test configurations.

7. Hadron resolution as a function of shower integration time for the 1" iron-scintillator test configuration.

8. Electromagnetic resolution as a function of inverse squareroot of energy for the three homogeneous test configurations.

9. Simulated and measured hadron shower depth profiles of 25 GeV pions in 3/4" iron-scintillator homogeneous test configuration. The solid histogram is simulation and each bin corresponds to one cell.

10. Simulated and measured hadron shower depth profiles of 100 GeV pions in 3/4" iron-scintillator homogeneous test configuration. The solid histogram is simulation and each bin corresponds to one cell.

11. Simulated and measured hadron shower depth profiles of 25 GeV pions in 3/4" lead-scintillator homogeneous test configuration. The solid histogram is simulation and each bin corresponds to one cell.

12. Simulated and measured hadron shower depth profiles of 100 GeV pions in 3/4" lead-scintillator homogeneous test configuration. The solid histogram is simulation and each bin corresponds to one cell.

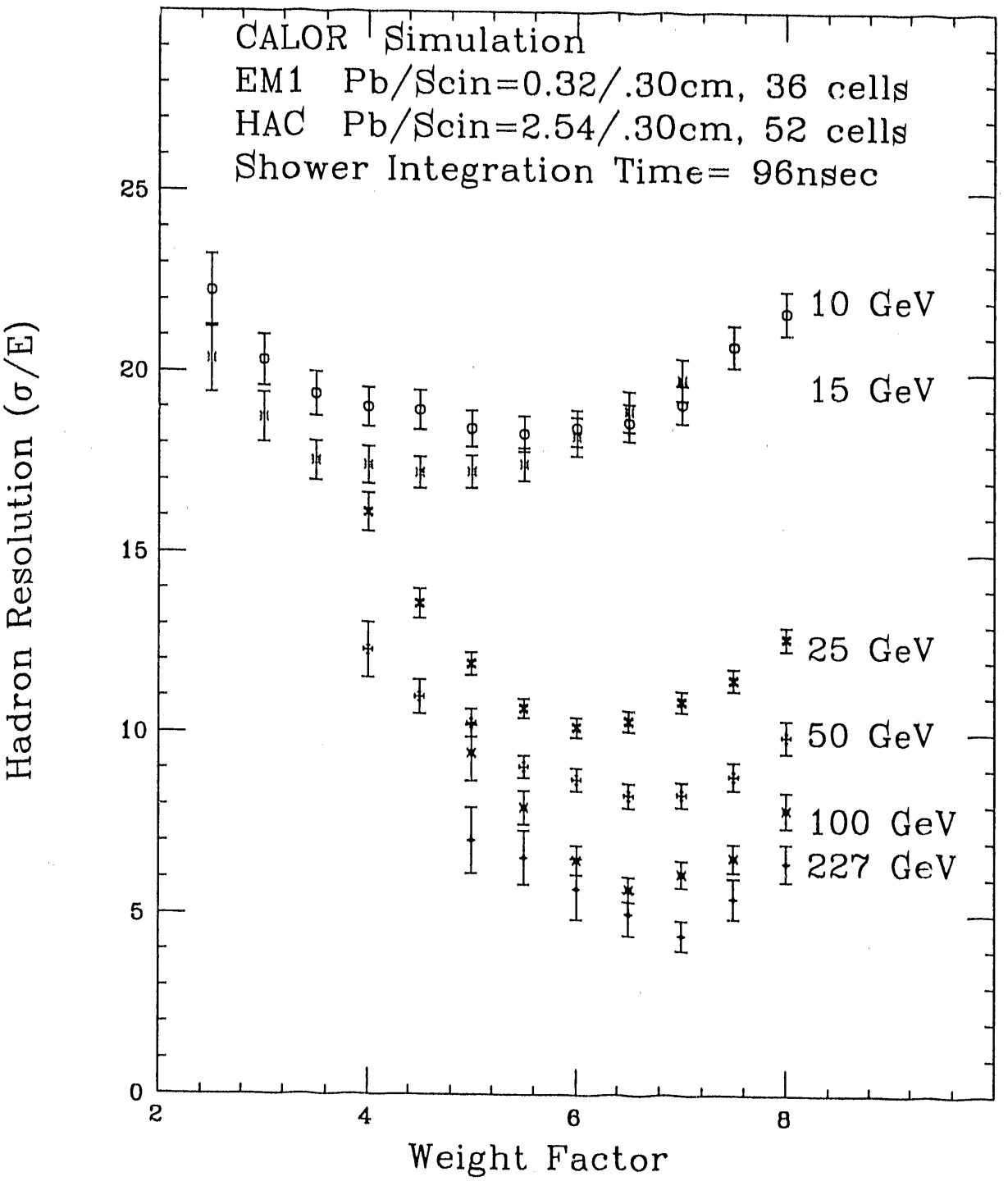
CALOR Simulation
EM1 Pb/Scin=0.32/.30cm, 36 cells
HAC Pb/Scin=2.54/.30cm, 52 cells
Shower Integration Time= 96nsec
10 GeV
15 GeV
25 GeV
50 GeV
100 GeV
227 GeV
Hadron Resolution (σ/E)
Weight Factor
0
5
10
15
20
25
2
4
6
8

Figure 1

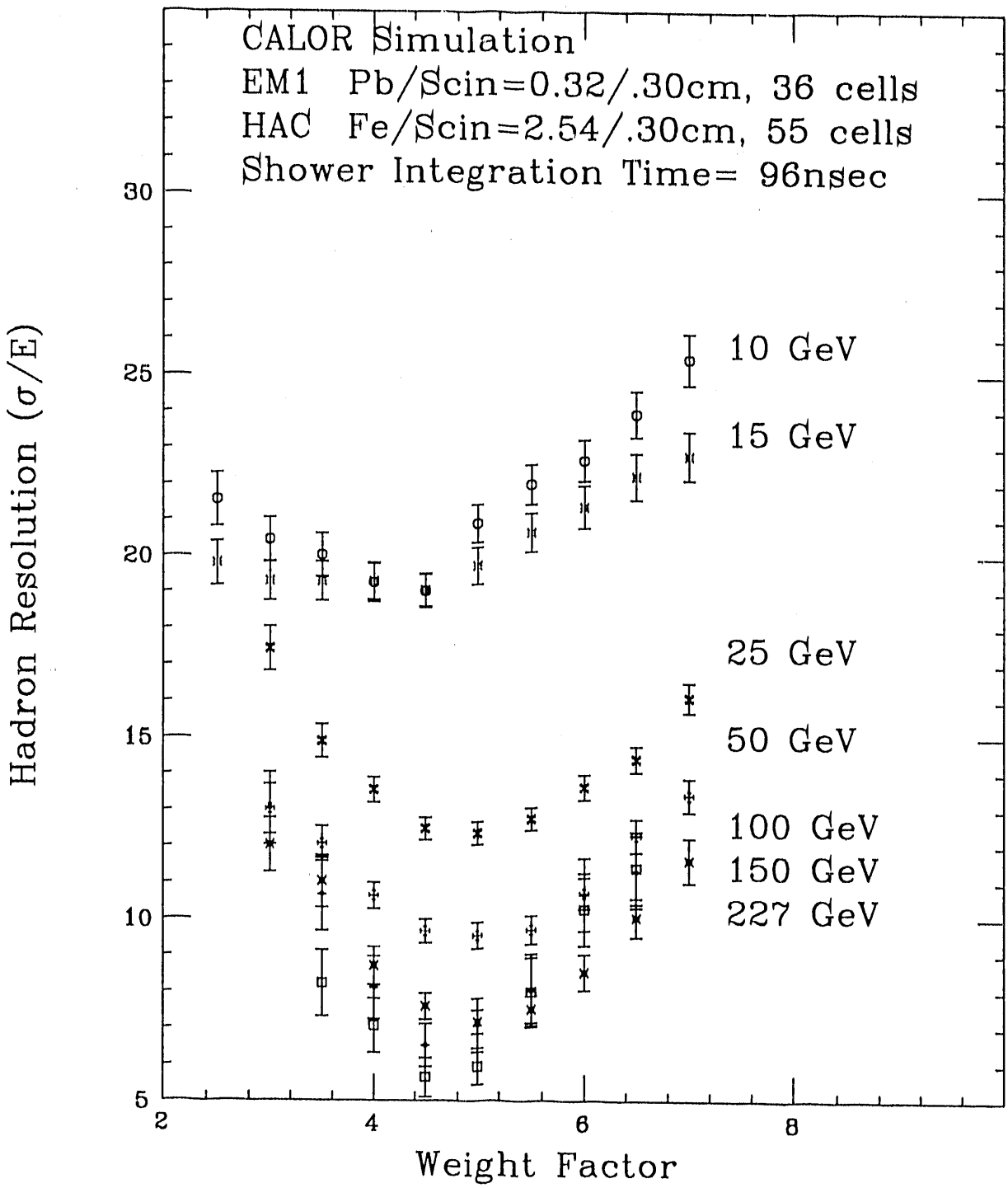
CALOR Simulation
EM1 Pb/Scin=0.32/.30cm, 36 cells
HAC Fe/Scin=2.54/.30cm, 55 cells
Shower Integration Time= 96nsec
10 GeV
15 GeV
25 GeV
50 GeV
100 GeV
150 GeV
227 GeV
Hadron Resolution (σ/E)
Weight Factor
30
25
20
15
10
5
2
4
6
8

Figure 2

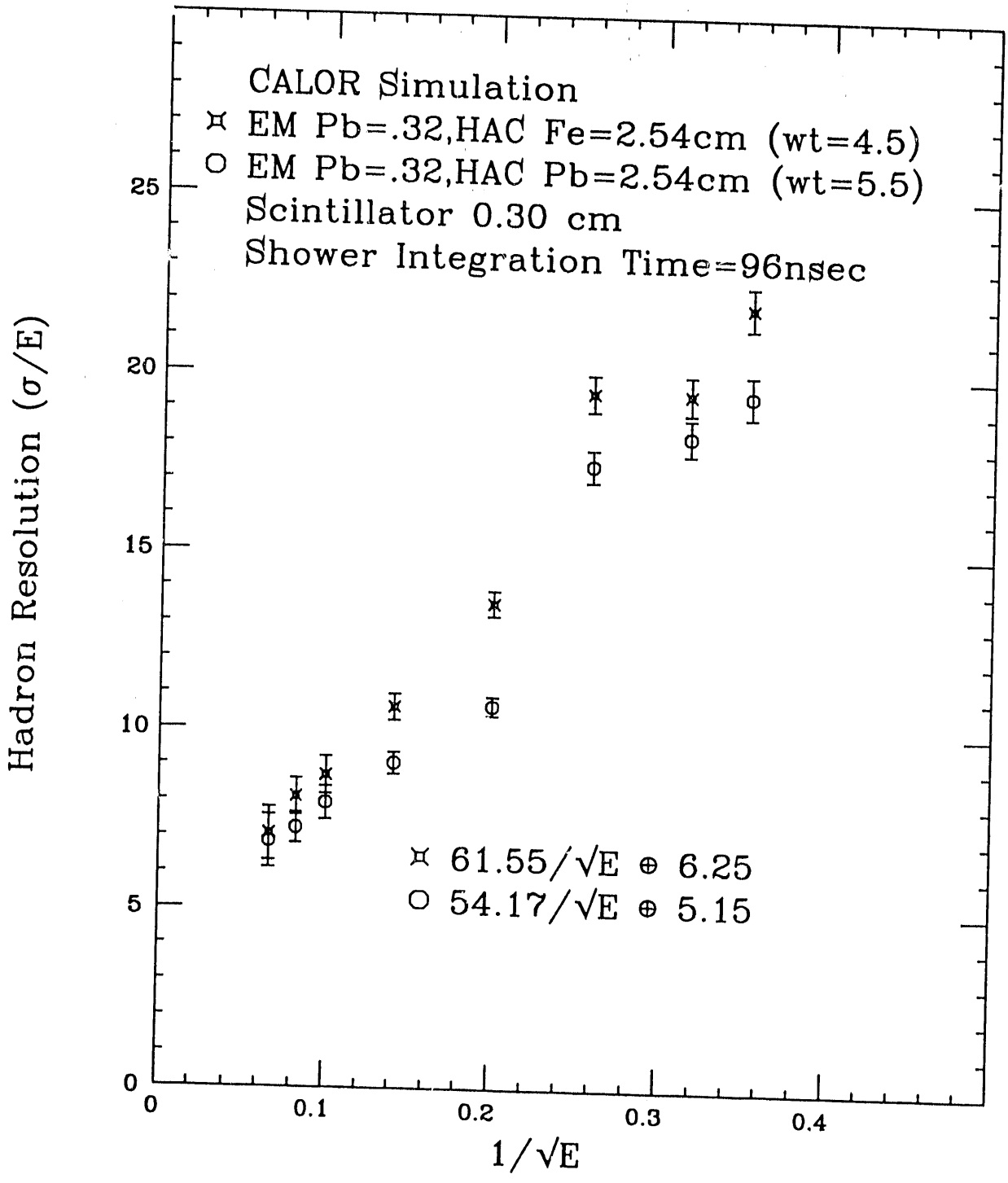
CALOR Simulation
EM Pb=.32,HAC Fe=2.54cm (wt=4.5)
EM Pb=.32,HAC Pb=2.54cm (wt=5.5)
Scintillator 0.30 cm
Shower Integration Time=96nsec
61.55/√E ⊕ 6.25
54.17/√E ⊕ 5.15
Hadron Resolution (σ/E)
1/√E
0
5
10
15
20
25
0.1
0.2
0.3
0.4

Figure 3

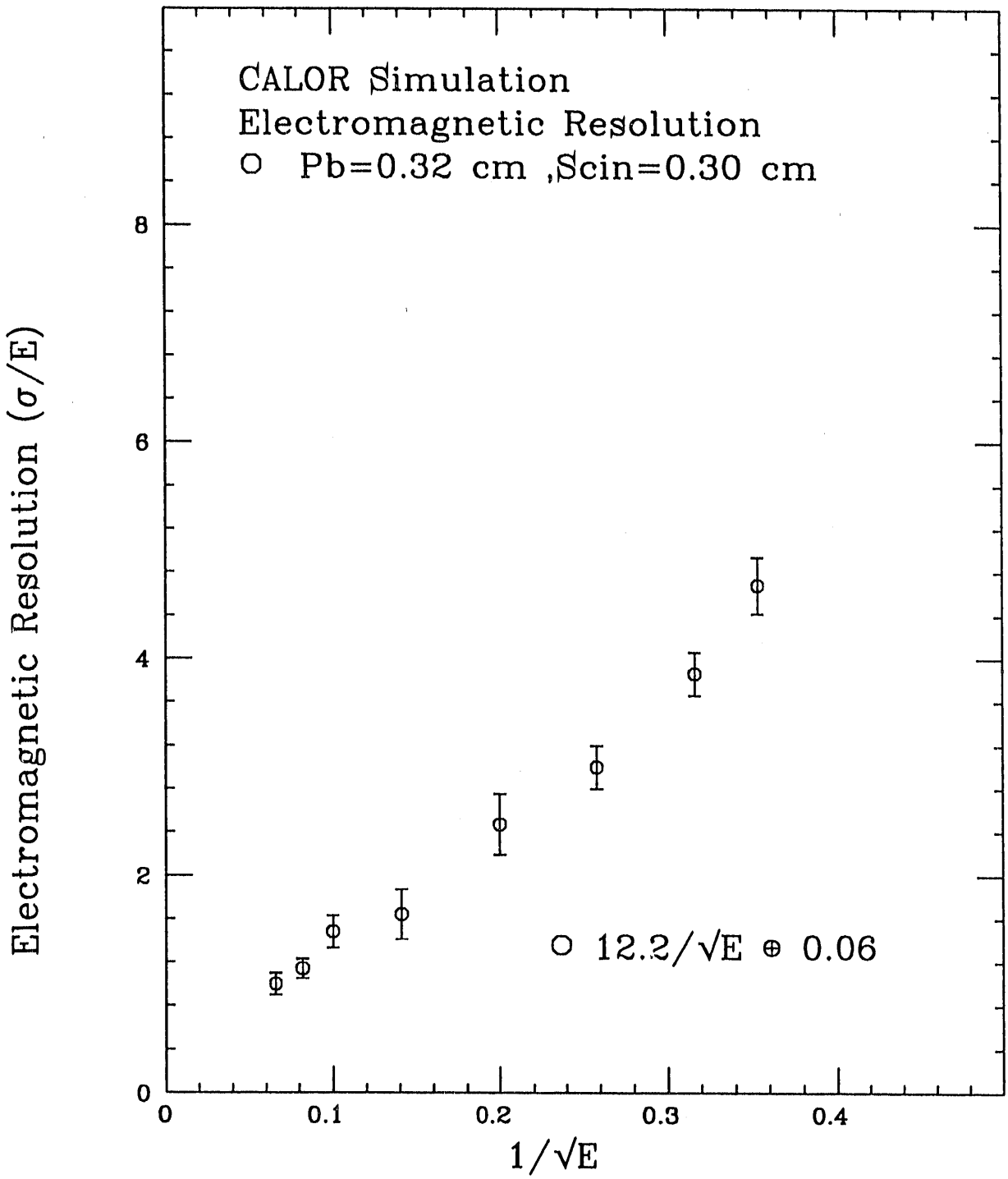
CALOR Simulation
Electromagnetic Resolution
○ Pb=0.32 cm ,Scin=0.30 cm
○ 12.2/√E ⊕ 0.06
Electromagnetic Resolution (σ/E)
1/√E
0
2
4
6
8
0
0.1
0.2
0.3
0.4

Figure 4

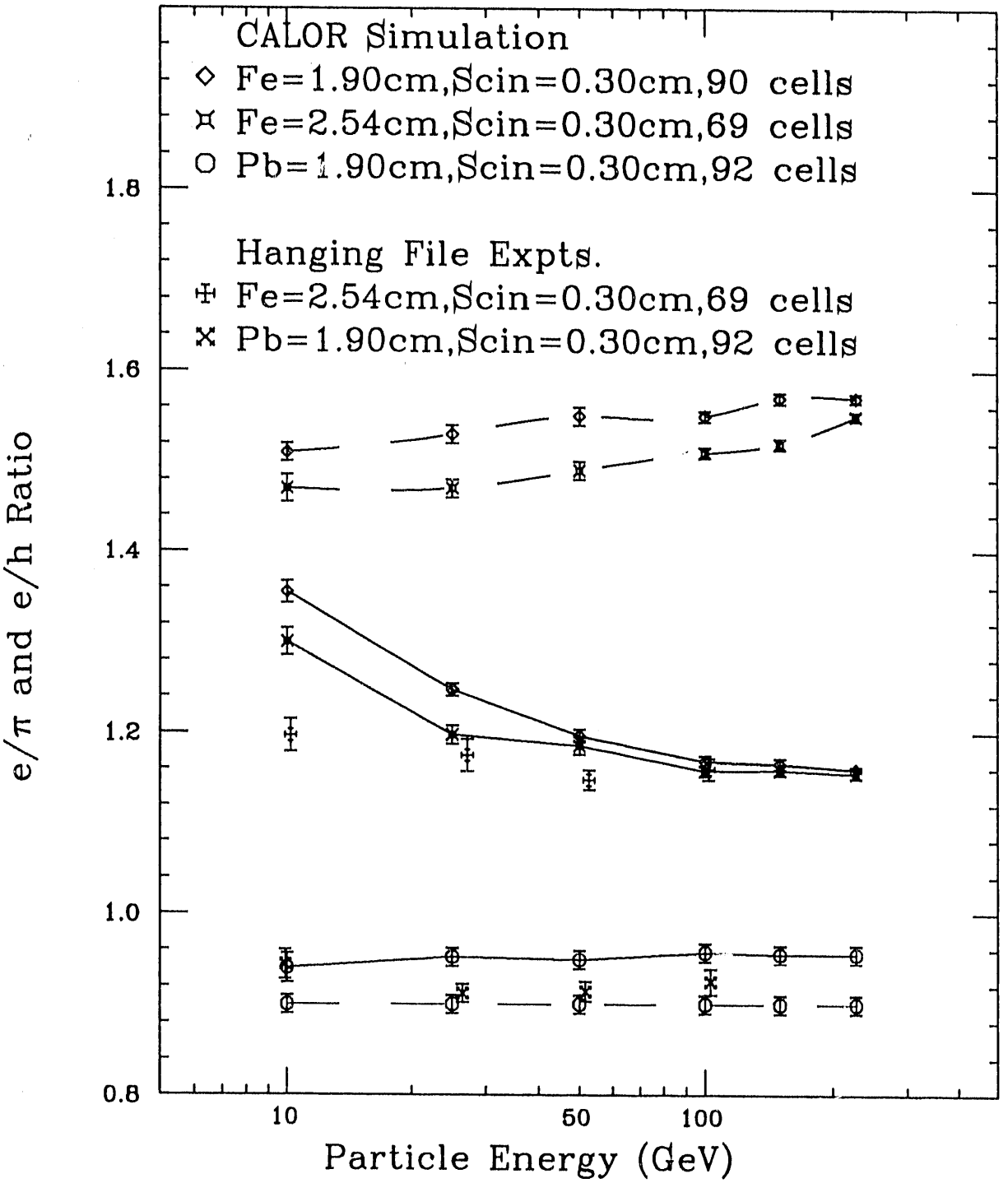
CALOR Simulation
Fe=1.90cm,Scin=0.30cm,90 cells
Fe=2.54cm,Scin=0.30cm,69 cells
Pb=1.90cm,Scin=0.30cm,92 cells
Hanging File Expts.
Fe=2.54cm,Scin=0.30cm,69 cells
Pb=1.90cm,Scin=0.30cm,92 cells
e/π and e/h Ratio
1.8
1.6
1.4
1.2
1.0
0.8
10
50
100
Particle Energy (GeV)

Figure 5

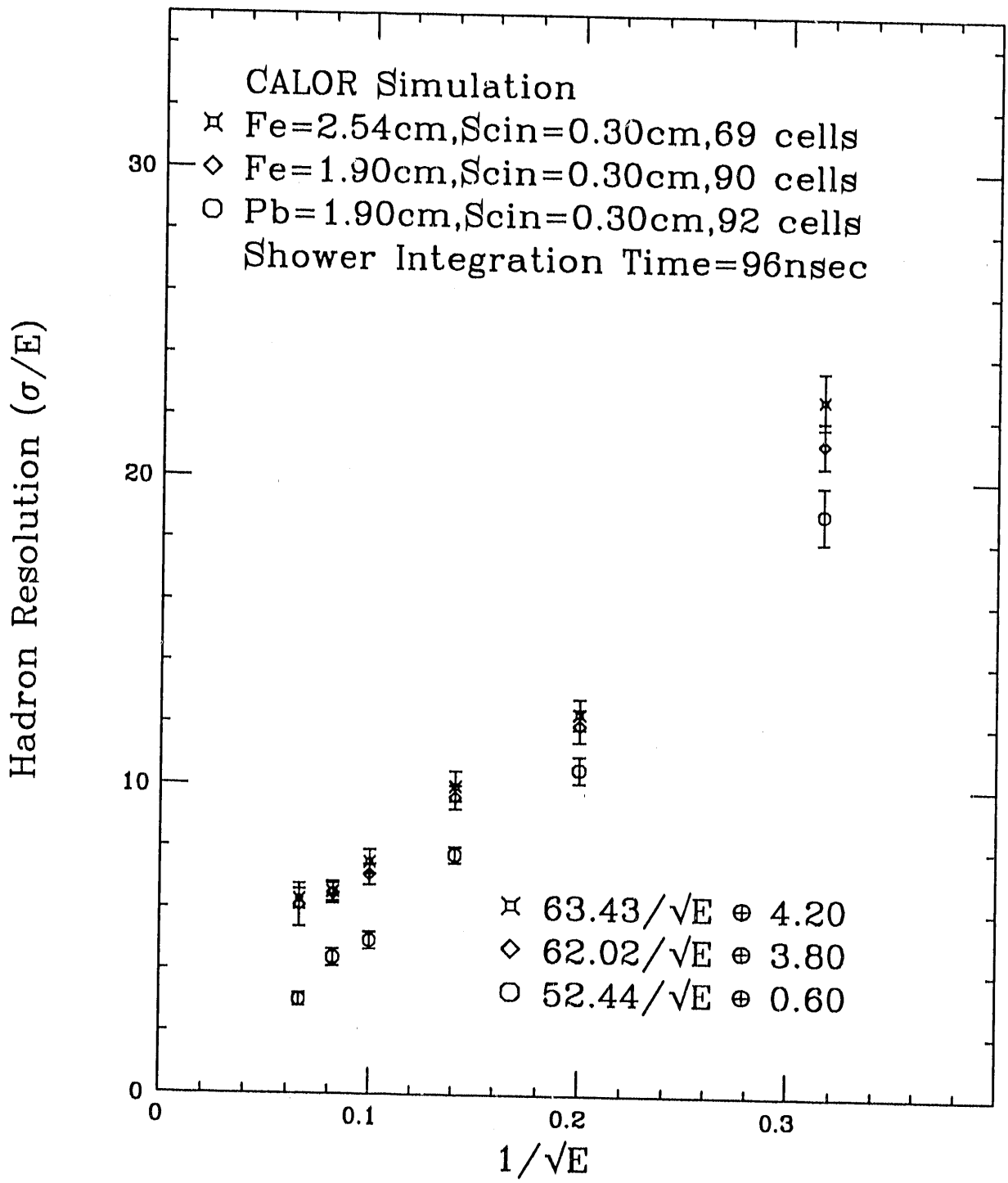
CALOR Simulation
Fe=2.54cm,Scin=0.30cm,69 cells
Fe=1.90cm,Scin=0.30cm,90 cells
Pb=1.90cm,Scin=0.30cm,92 cells
Shower Integration Time=96nsec
63.43/√E ⊕ 4.20
62.02/√E ⊕ 3.80
52.44/√E ⊕ 0.60
Hadron Resolution (σ/E)
1/√E
0
10
20
30
0.1
0.2
0.3

Figure 6

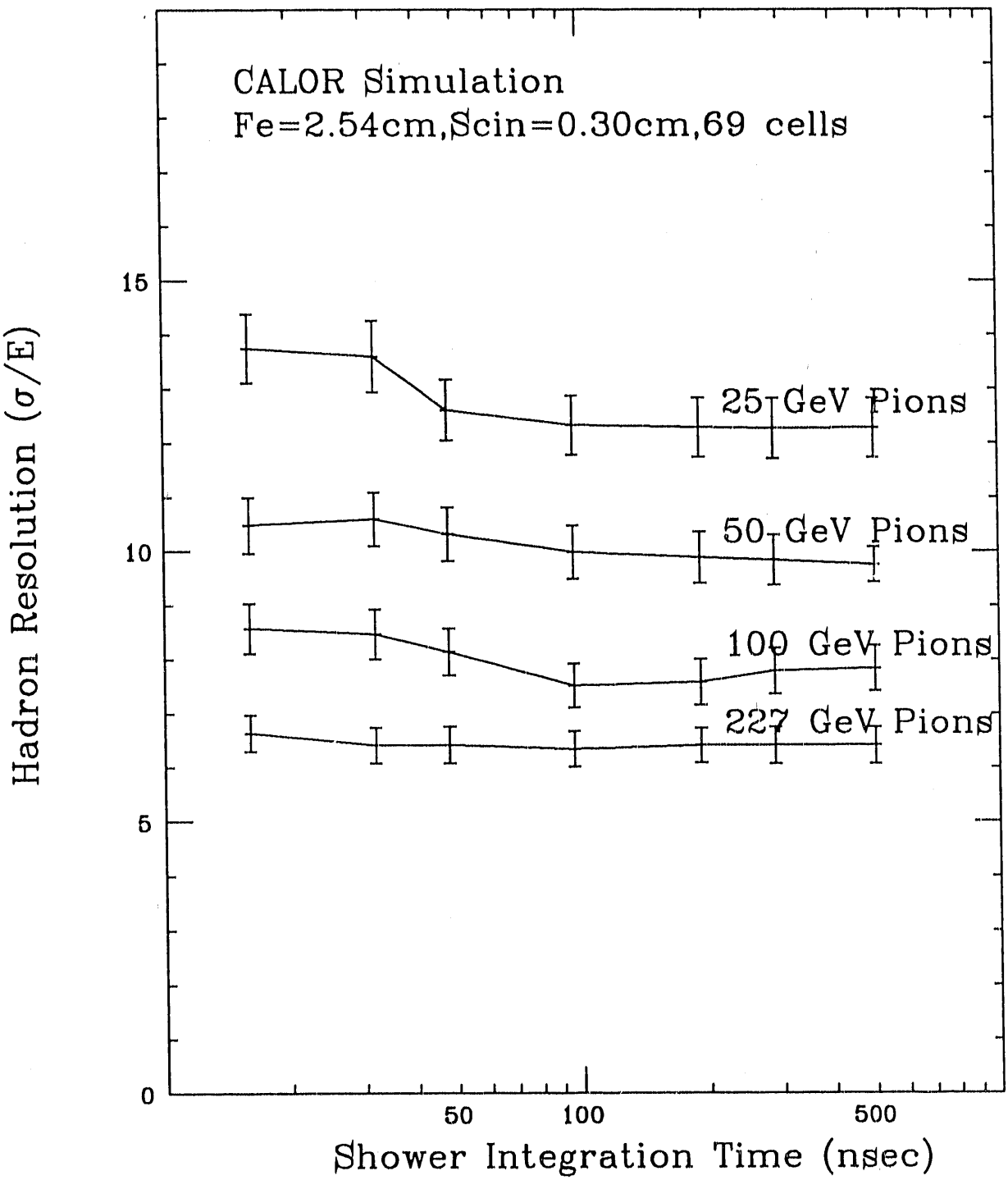
CALOR Simulation
Fe=2.54cm,Scin=0.30cm,69 cells
25 GeV Pions
50 GeV Pions
100 GeV Pions
227 GeV Pions
Hadron Resolution (σ/E)
0
5
10
15
50
100
500
Shower Integration Time (nsec)

Figure 7

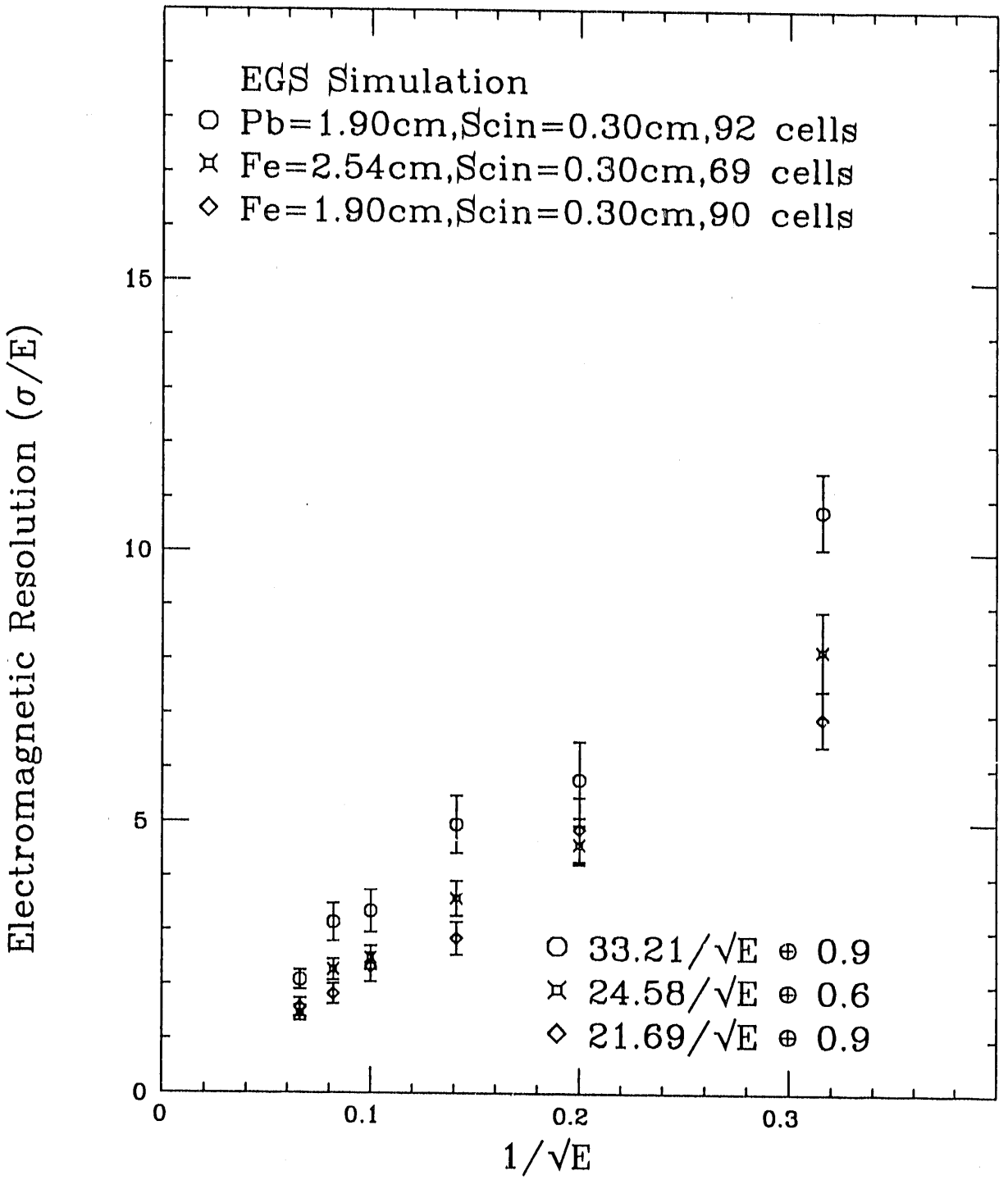
EGS Simulation
Pb=1.90cm,Scin=0.30cm,92 cells
Fe=2.54cm,Scin=0.30cm,69 cells
Fe=1.90cm,Scin=0.30cm,90 cells
33.21/√E ⊕ 0.9
24.58/√E ⊕ 0.6
21.69/√E ⊕ 0.9
Electromagnetic Resolution (σ/E)
1/√E
0
5
10
15
0.1
0.2
0.3

Figure 8

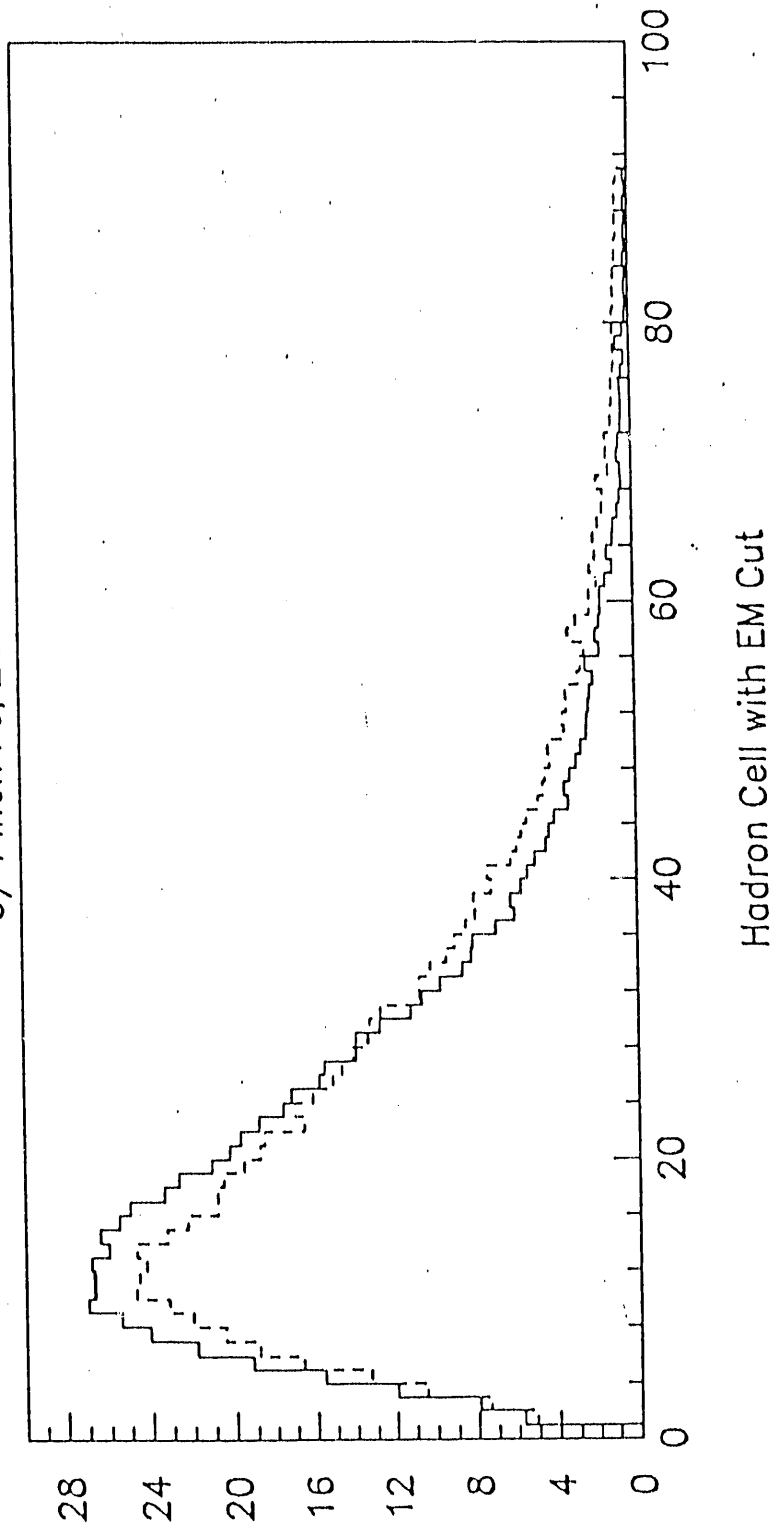
3/4 inch Fe, 25 GeV
Hadron Cell with EM Cut
0
4
8
12
16
20
24
28
0
20
40
60
80
100

Figure 9

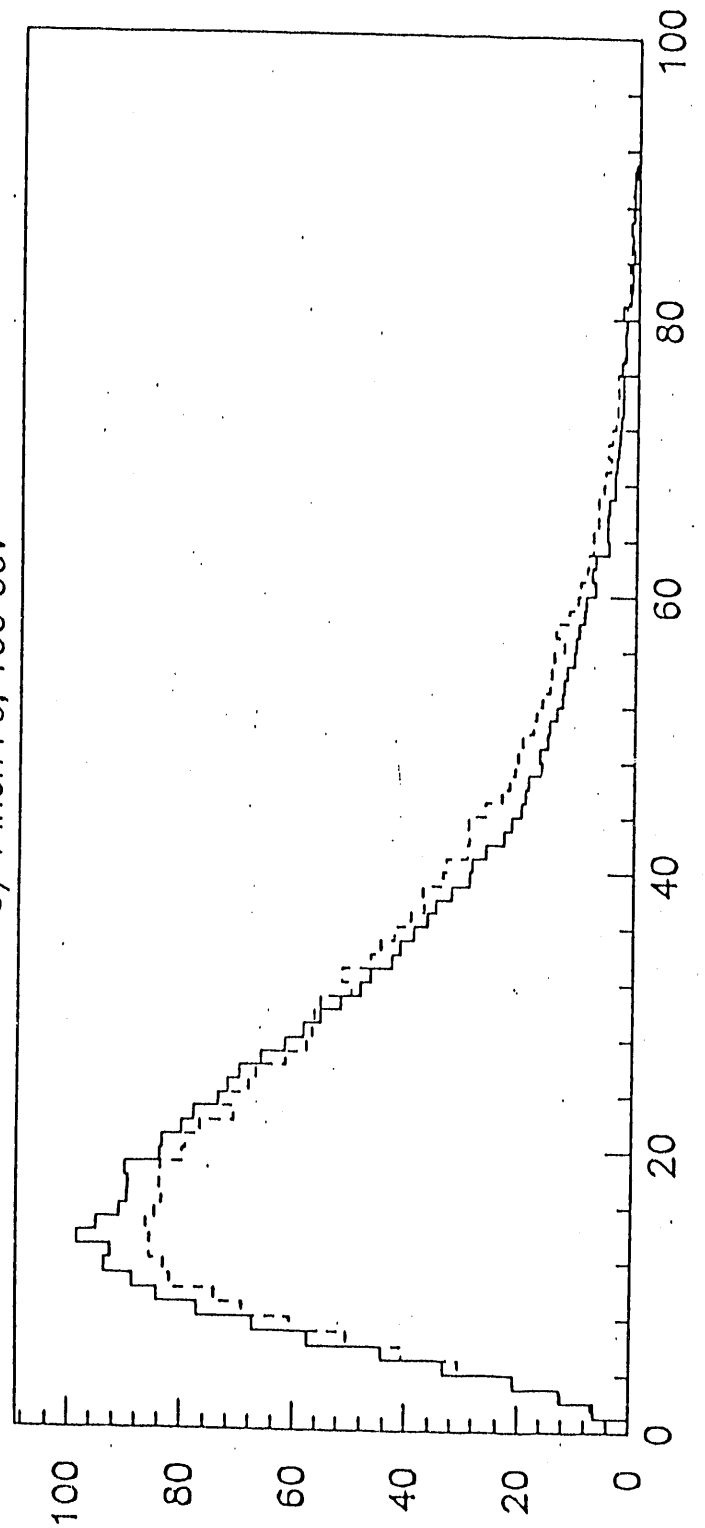
3/4 inch Fe, 100 GeV
Hadron Cell with EM Cut
0
20
40
60
80
100
0
20
40
60
80
100

Figure 10

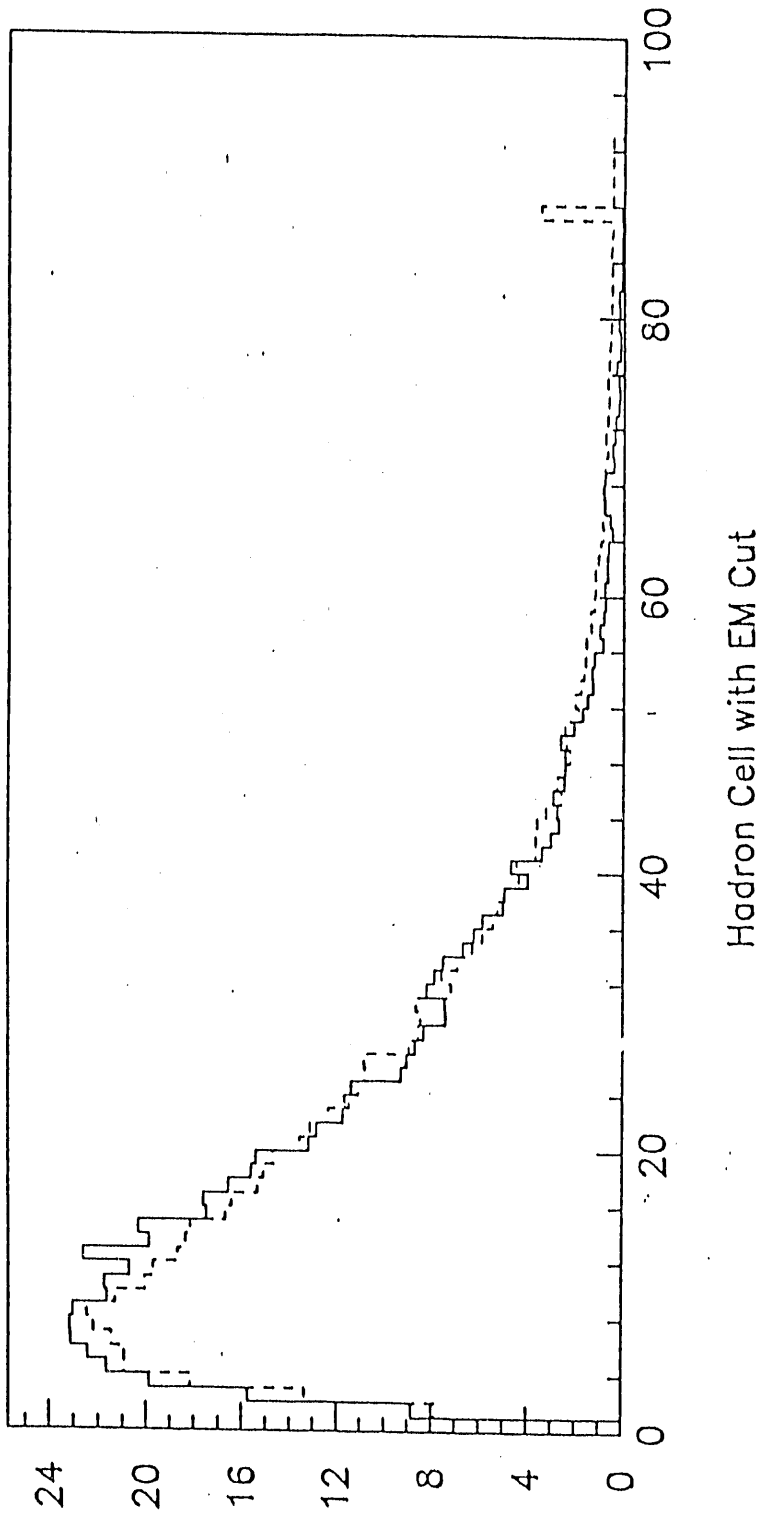
3/4 inch Pb, 25 GeV
Hadron Cell with EM Cut
0
4
8
12
16
20
24
0
20
40
60
80
100

Figure 11

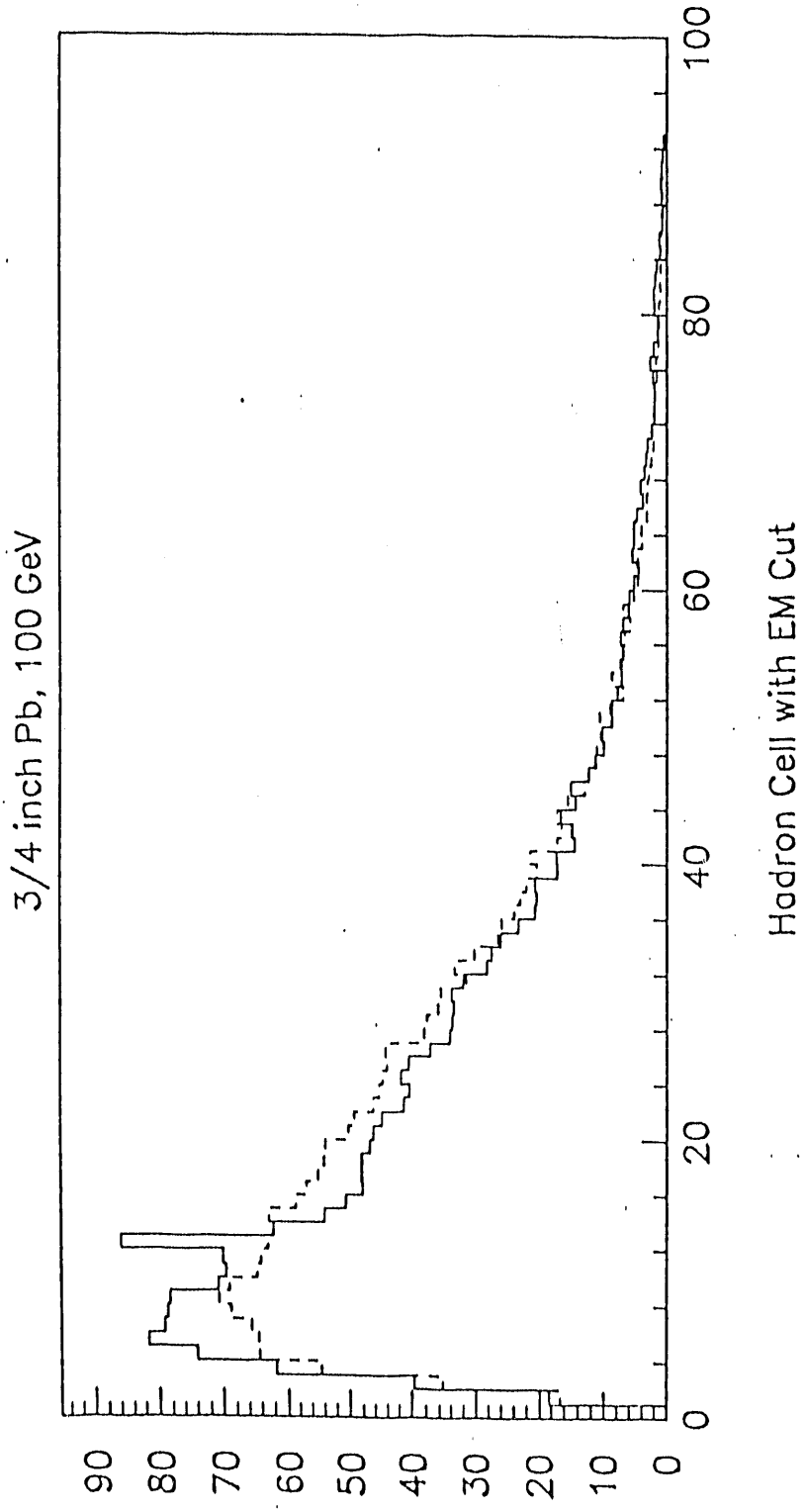
3/4 inch Pb, 100 GeV
Hadron Cell with EM Cut
0
20
40
60
80
100
0
10
20
30
40
50
60
70
80
90

Figure 12

DATE
FILMED
7/15/92